

Preferential Batch Bayesian Optimization

Eero Siivola¹, Akash Kumar Dhaka¹, Michael Riis Andersen²,
 Javier González³, Pablo García Moreno³, Aki Vehtari¹

¹Aalto University, ² Amazon.com, ³ Department of Applied Mathematics
 and Computer Science, Technical University of Denmark

Abstract

Most research in Bayesian optimization (BO) has focused on *direct feedback* scenarios, where one has access to exact, or perturbed, values of some expensive-to-evaluate objective. This direction has been mainly driven by the use of BO in machine learning hyper-parameter configuration problems. However, in domains such as modelling human preferences, A/B tests or recommender systems, there is a need of methods that are able to replace direct feedback with *preferential feedback*, obtained via rankings or pairwise comparisons. In this work, we present Preferential Batch Bayesian Optimization (PBBO), a new framework that allows to find the optimum of a latent function of interest, given any type of parallel preferential feedback for a group of two or more points. We do so by using a Gaussian process model with a likelihood specially designed to enable parallel and efficient data collection mechanisms, which are key in modern machine learning. We show how the acquisitions developed under this framework generalize and augment previous approaches in Bayesian optimization, expanding the use of these techniques to a wider range of domains. An extensive simulation study shows the benefits of this approach, both with simulated functions and four real data sets.

1 Introduction

Understanding and emulating the way intelligent agents make decisions is at the core of what machine learning and artificial intelligent aims to achieve. To fulfill this goal, behavioural features can be learned from demonstrations like when a robot arm is trained using human generated examples [Ho and Ermon, 2016]. In many cases, however, the

optimality of the instances is questionable. Reinforcement learning, via the explicit definition of some reward, is another approach [Sutton and Barto, 1998]. That can be, however, subject to biases. Imagine asking a user of a streaming service to score a movie between zero and ten. Implicitly, this question assumes that he/she has a sense of the scale in which the new movie is evaluated, which implies that a detailed exploration of the *movies space* has been already carried out.

An alternative way to understanding agents decisions is to do it via preferences. In the movies example any two movies can be compared without any scale. Also the best of ten movies can be selected or a group of movies can be ranked from the worst to the best. This feedback, which can be provided without sense of scale, provides information about the user preferences. Indeed, in prospect theory several studies have demonstrated that humans are better at evaluating differences rather than absolute magnitudes [Kahneman and Tversky, 1979]. This idea is not new in machine learning and it has been applied in recommender systems [Brusilovsky et al., 2007], the ranking of game players skills [Herbrich et al., 2007] and to evaluate strategies in reinforcement learning.

In the Bayesian optimization literature (BO), these ideas have also been studied in cases where the goal is to learn the optimum of some latent preference function defined in some Euclidean space [Chu and Ghahramani, 2005b, González et al., 2017]. Available methods use pairwise comparisons to recover a latent preference function, which in turn is used to make decisions about new queries. Despite the *batch* setting being a natural scenario here, where more than two points in the space are compared at once, it has not yet been carefully studied in the literature. One relevant example for batch feedback is product design, especially in the food industry, where one can only produce a relatively small batch of different products at a time. The quality of products, especially for foods, is usually highly dependent on the time since production. The whole batch is usually best to be evaluated at once and the next batch of products should be designed based on the feedback so far. In this work, we show that robust mechanisms to propose preferential batches

sequentially are very useful in practice, but far from trivial to define.

1.1 Problem formulation

Let $f : \mathcal{X} \rightarrow \mathbb{R}$ be a well-behaved *black-box* function defined on a bounded subset $\mathcal{X} \subseteq \mathbb{R}^d$. We are interested in solving the global optimization problem of finding

$$\mathbf{x}_{\min} = \arg \min_{\mathbf{x} \in \mathcal{X}} f(\mathbf{x}). \quad (1)$$

We assume that f is not directly accessible and that (noisy) queries to f can only be done in batches $\mathcal{B} = \{\mathbf{x}_i \in \mathcal{X}\}_{i=1}^q$. We assume that f is evaluated at all the batch locations, $f(\mathbf{x}_i)$, $i = 1, \dots, q$, and we can receive a set of pairwise preferences of the evaluations. We denote a pairwise preference by $\mathbf{x}_i \prec \mathbf{x}_j := f(\mathbf{x}_i) \leq f(\mathbf{x}_j)$. The goal is to find \mathbf{x}_{\min} by limiting the total number of batch queries to f , which are assumed to be expensive. This setup is different to the one typically used in BO where direct feedback from (noisy) evaluations of f is available [Jones, 2001, Snoek et al., 2012].

In particular, we are interested in cases in which the preferential feedback is collected in a sequence of B batches $\mathcal{B}_b = \{\mathbf{x}_i \in \mathcal{X}\}_{i=1}^q$ for $b = 1, \dots, B$. Within each batch, at iteration b , the feedback is assumed to be collected as a complete (or partial) ordering of the elements of the batch, $I \in \mathbb{N}^q$, s.t. $\mathbf{x}_{I_i}^b \prec \mathbf{x}_{I_j}^b$, $\forall i < j \leq q$ or by the selection of the preferred element \mathbf{x}_i^b of the batch $\mathbf{x}_i^b \prec \mathbf{x}_j^b \forall j \neq i$.

Since all batch locations are assumed to be evaluated at once it is always true that if $\mathbf{x}_1^b \prec \mathbf{x}_2^b$ and $\mathbf{x}_2^b \prec \mathbf{x}_3^b$ at iteration b it follows that $\mathbf{x}_1^b \prec \mathbf{x}_3^b$. However, due to the noise in the evaluations, this cannot be generalised across batches as $f(\mathbf{x}_i^k) \neq f(\mathbf{x}_j^l)$ even if $\mathbf{x}_i^k = \mathbf{x}_j^l$. Within a batch, the feedback stays the same if comparisons of type $\mathbf{x}_1^b \prec \mathbf{x}_3^b$ are removed. A valid batch feedback can be thought as a directed acyclic graph (DAG) and removing unnecessary comparisons is same as performing transitive reduction to the DAG. Most common feedbacks, such as complete ordering, partial ordering or the batch winner approach can be presented with at most $q - 1$ pairwise comparisons.

We concentrate mainly on the batch winner case in this work. We argue that the batch winner feedback is the most useful type of batch feedback. As the preferential feedback is collected from humans, full ranking of the batch is laborious for large batches and it sometimes even is impossible (e.g. in A/B testing). Full ranking can also be reduced to the batch winner case. In addition, as we later demonstrate in the experiments, the added benefit of full ranking instead of batch winner is very small for BO.

1.2 Related work and contributions

Pairwise comparisons are usually called *duels* in the BO and bandits literature. In the BO context, Chu and Ghahramani [2005b] introduced a likelihood for including preferential feedback into Gaussian processes (GPs). Chu and Ghahramani [2005a] recomputed the model for all possible duel outputs of a discrete dataset and used the expected entropy loss to select the next query. Brochu [2010] used expected improvement (EI, Močkus [1975]) sequentially to select the next duel. Most recently, González et al. [2017] introduced a new state of the art and non heuristic method inspired by Thompson sampling to select the next duel. In the bandits literature, Yue and Joachims [2009] were the first one to study pairwise comparisons, or duelling bandits. Yuea et al. [2012] were the first to study the optimization methods of the duelling bandits. The current state-of-the art duelling bandits algorithm by Sui et al. [2017] is based on Thompson sampling (TS).

In this work we introduce a method called *preferential batch Bayesian optimization* (PBBO) that allows optimizing black-box functions with BO when one can query preferences in a batch of input locations. The main contributions are:

- We formulate the problem in such a way that the model for latent inputs in preference feedback scales beyond a batch size of two.
- We present and compare three alternative inference methods for the intractable posterior that results from the proposed batch setting with the batch winner feedback.
- We present three theoretically justified acquisition methods and practical ways of computing them.
- We compare all inference methods, acquisition functions and batch sizes jointly in extensive experiments with simulated and real data and provide recommendations to practitioners.

The code for reproducing the results is available at https://github.com/EmuKit/emuikit/tree/master/emuikit/examples/preferential_batch_bayesian_optimization

The remainder of the paper is organized as follows. In Section 2, we introduce the theoretical background. In Section 3, we introduce batch input preferential Bayesian optimization and three new acquisition functions. In Section 4 we show the benefits of our approach with simulated case studies and real data. We conclude the paper with discussion in Section 5.

2 Modeling batch preferential feedback with Gaussian processes

We assume that the latent black box function f is a realization of a zero-mean Gaussian process (GP), $p(f) = \mathcal{GP}$ fully specified by some covariance function K [Rasmussen and Williams, 2006]. The covariance function specifies the covariance of the latent function between any two points.

2.1 Likelihood for pairwise comparisons

Chu and Ghahramani [2005b] proposed the following likelihood for pairs of preferential observations.

$$p(\mathbf{x}_i \prec \mathbf{x}_j | f_i, f_j) = \iint \mathbb{1}_{y_i < y_j} N(y_i | f_i, \sigma^2) N(y_j | f_j, \sigma^2) dy_i dy_j = \Phi(z_{ij}), \quad (2)$$

where $z_{ij} = \frac{f_j - f_i}{\sqrt{2}\sigma}$, $\Phi(z) = \int_{-\infty}^z N(\gamma | 0, 1) d\gamma$ and f_i is latent function value at \mathbf{x}_i and σ is the noise of the comparison. As the likelihood is not Gaussian, the posterior distribution is intractable and some posterior approximation has to be used.

2.2 Likelihood for batches of preferences

We propose a new likelihood function to capture the comparisons that are collected in batches. Assuming the general case of batch \mathcal{B} of q locations and a list $\mathbf{C} \in \mathbb{N}^{m \times 2}$, such that $\mathbf{x}_{C_{i,1}} \prec \mathbf{x}_{C_{i,2}} \forall i \in [1, \dots, m]$, the likelihood of the preferences is

$$p(\mathbf{C} | \mathbf{f}) = \int \dots \int \left(\prod_{i=1}^m \mathbb{1}_{y_{C_{i,1}} \leq y_{C_{i,2}}} \right) \left(\prod_{k=1}^q N(y_k | f_k, \sigma^2) \right) dy_1 \dots dy_q. \quad (3)$$

If the provided feedback is only the batch winner \mathbf{x}_j , the likelihood can be further simplified to

$$p(\mathbf{C} | \mathbf{f}) = \int N(y_j | f_j, \sigma^2) \prod_{i=1, i \neq j}^q \Phi \left(\frac{y_j - f_i}{\sigma} \right) dy_j. \quad (4)$$

Note that this is not same as product of Equations (2) across all pairwise comparisons, as the uncertainty of the batch winner needs to be taken jointly into account.

2.3 Posterior probabilities

The posterior distribution and the posterior predictive distributions of the model outcome are needed for making reasoned decisions based on the existing data. Let us assume B preference outcome observations $\mathbf{C}^b \in \mathbb{N}^{m \times 2}$ at batches $\mathbf{X}^b \in \mathbb{R}^{q \times d}$ ($b = 1, \dots, B$). Let us assume that the unknown latent function values $\mathbf{f}^b \in \mathbb{R}^{q \times 1}$ ($b = 1, \dots, B$)

have a GP prior and each batch of preferences are conditionally independent given the latent values \mathbf{f}^b at \mathbf{X}^b .

$$p(\{\mathbf{C}^b\}_{b=1}^B | \{\mathbf{f}^b\}_{b=1}^B) = \prod_{b=1}^B p(\mathbf{C}^b | \mathbf{f}^b).$$

The joint posterior distribution of all the latent function values $\{\mathbf{f}_b^p\}_{b=1}^B$ and \mathbf{f}^* (at unseen locations \mathbf{X}^*) is then

$$p(\mathbf{f}^*, \{\mathbf{f}^b\}_{b=1}^B | \mathbf{X}^*, \{\mathbf{X}^b\}_{b=1}^B, \{\mathbf{C}^b\}_{b=1}^B) \propto p(\mathbf{f}^*, \{\mathbf{f}^b\}_{b=1}^B | \mathbf{X}^*, \{\mathbf{X}^b\}_{b=1}^B) \prod_{b=1}^B p(\mathbf{C}^b | \mathbf{f}^b). \quad (5)$$

The posterior predictive distribution for \mathbf{f}^* is obtained by integrating over $\{\mathbf{f}^b\}_{b=1}^B$.

2.4 Model selection and inference

Since the likelihood of the preferential observations is not Gaussian, the whole posterior distribution is intractable and some approximation has to be used. Next we present expectation propagation (EP) and variational inference (VI) approximations. EP can be used for general batch feedback in Equation (3). With VI we limit to the batch winner case in Equation (4) as we argue it to be the most useful type of batch feedback.

2.4.1 Expectation propagation using multivariate normal as an approximate distribution

EP [Opper and Winther, 2000, Minka, 2001] approximates some untractable likelihood by a distribution from the exponential family, so that the Kullback–Leibler (KL) divergence from the posterior marginals to the approximative posterior marginals is minimized. In this paper, we use multivariate normal distributions for each batch so that in the posterior distribution in Equation (5), $\prod_{b=1}^B p(\mathbf{C}^b | \mathbf{f}^b)$ is approximated by $\prod_{b=1}^B N(\mathbf{f}^b | \boldsymbol{\mu}^b, \boldsymbol{\Sigma}^b)$. In practice, for approximative distributions from the exponential family, this can be done in an iterative manner where approximation of batch b is replaced by the original one and the approximation of batch b is updated by matching the mean and variance of the full approximative distribution and the replaced one. Since the moments for the distribution in Equation (3) are not analytically available, we approximate them by sampling.

2.4.2 Variational Inference using stochastic gradient descent

The pairwise comparison likelihood (Equation (2)) has the same structure as the one-vs-each likelihood (OVE) proposed by Titsias [2016]. This approximation, introduced in context of multiclass classification with linear models, was also used by Villacampa-Calvo and Hernández-Lobato [2017] for GP models. The OVE formulation simplifies

multiclass classification to pairwise comparisons between the winner class label and rest of the classes. Given the batch winner, we can formulate feedback as pairwise duels between two observations in a batch. However, this is not an exact likelihood, but a lower bound since we do not integrate over the uncertainty of the batch winner.

Let \mathbf{K} be the prior covariance matrix at $\mathbf{X} = [\mathbf{X}^1, \dots, \mathbf{X}^B]^T$, α a vector and \mathbf{L} a lower triangular matrix. Also, let $\mathbf{f} = [\mathbf{f}^1, \dots, \mathbf{f}^B]^T$. Following Opper and Archambeau [2009], we then posit a Gaussian approximation of the posterior, the optimal form for which in terms of KL divergence is given by

$$q(\mathbf{f}) = N(\mathbf{f} | \mathbf{K}\alpha, \mathbf{L}\mathbf{L}^T). \quad (6)$$

The mean vector is parameterised as $\mathbf{K}\alpha$ and as the posterior covariance needs to be positive definite, $\mathbf{L}\mathbf{L}^T$ is used.

Alternatively, if the covariance matrix is parametrized using the vector β instead, then the posterior can be formulated as

$$q(\mathbf{f}) = N(\mathbf{f} | \mathbf{K}\alpha, (\mathbf{K} + \mathbf{I}\beta)^{-1}), \quad (7)$$

where there are only $2N$ parameters to optimize.

In both approaches the variational parameters are optimised in an inner loop with stochastic gradient descent (SGD) optimization after collecting derivatives and likelihood terms from each pairwise comparison. The benefit of this form compared to EP is that it gives us a single bound making the optimization easier.

3 Sequential learning for batch settings

In this section, we present three strategies for selecting the batch locations jointly. Two first acquisition strategies are theoretically justified, but slow to compute, and the third is more heuristic but faster. To maintain readability, we present the formulas only for the batch winner type preferences in Equation (4). However, we show how these formulas could be extended to the general case in Section 3.4. Last in this section, we show the general algorithm for performing preferential batch Bayesian optimization.

3.1 Expected Improvement for preferential batches

Expected improvement is a well established exploitative acquisition function that computes the expected improvement over the minimum of the values observed so far and that also has an extension in the batch setting, batch EI (q-EI) [Chevalier and Ginsbourger, 2013]. In the context of preferential feedback, it is not possible to know the exact value of the current best y_{min} . This adds one more source of uncertainty to the regular q-EI for batches of direct feedback. In the context of our work, preferential q-EI (pq-EI) becomes

$$pq\text{-EI} = \mathbb{E}_{\mathbf{y}, \mathbf{y}_{min}} \left[\left(\max_{i \in [1, \dots, q]} (y_{min} - y_i) \right)_+ \right]. \quad (8)$$

In our batch setting, pq-EI cannot be computed in closed form and the computational cost of numerical integration becomes higher as the number of performed iterations increases. See Appendix A1 for further details.

One way to avoid the high computational cost caused by the uncertainty in y_{min} is to use some proxy for it that is easier to compute. González et al. [2016] presented the concept of Copeland expected improvement, where the improvement is computed over (soft) Copeland score at a location \mathbf{x} . However, since the joint distribution of the Copeland scores do not follow multivariate normal, computing them require updating the posterior of the model for every possible outcome of the comparison. Details of this can be found in the Appendix A2.

Another way of avoiding the high computational cost of having to integrate over the uncertainty of the minimum and not having to update the model posterior, is to use the minimum of the mean of the latent posterior ($\min_i \mu(\mathbf{x}_i)$) of the training data as a proxy for y_{min} and use the relatively fast q-EI

$$\begin{aligned} q\text{-EI} = \sum_{i=1}^q \mathbb{E}_{\mathbf{y}} & \left(\mu_{min} - y_i \mid y_i \leq y_{min}, y_i \prec y_j \forall j \neq i \right) \\ & p(y_i \leq \mu_{min}, y_i \leq y_j \forall j \neq i). \end{aligned} \quad (9)$$

Despite the acquisition function having no closed form solution, both the acquisition function value and its gradients can efficiently be approximated by using re-parameterisation trick of Kingma and Welling [2013] and some stochastic gradient descent algorithm. This way the variance of the gradient estimation is small enough for practical optimization even for relatively small number of samples from the posterior predictive distribution of the GP.

Each optimization step requires prediction and gradients of mean and full covariance at q locations. Assuming that we have observed N batches so far, this results to time complexity of $\mathcal{O}((Nq)^2 q(d+1)) = \mathcal{O}((N^2 q^3(d+1))$ per posterior sample per iteration. To make it more obvious, optimization of the acquisition function scales quadratically as a function of iterations, cubically as a function of batch size and linearly as a function of dimensionality of the optimization space. In practice, despite the number of posterior draws is relatively small thanks to the re-parameterisation trick, the algorithm becomes impractically slow for high dimensions or large batch sizes. Furthermore, the higher dimensional the optimization space ($q \times d$) is, the more (random) restarts the stochastic optimization of the batch locations requires to converge to the global optimum. In later phases of the optimization, the acquisition function also becomes very flat, causing the problem of vanishing gradients. Because of these issues, the optimization of the batch locations becomes slower at each BO iteration and we have less confidence of having obtained the true acquisition function maximum.

3.2 Pure exploration

González et al. [2016] show that in preference setting, querying locations that have most uncertain preference outcomes might lead to querying same locations multiple times. This also applies to the batch setting (see Appendix A3 for details). A better exploration strategy is to query preferences for which the probability of the outcome is most uncertain. Let us assume unseen locations $\mathbf{X}^* \in \mathcal{R}^{q \times d}$ with latent values \mathbf{f}^* . For the batch winner case the exploration strategy can be formulated as maximizing the sum of variances

$$\sum_{i=1}^q \text{Var}(p(y_i \leq y_j \forall j \neq i \mid \mathbf{f}^*)) = \sum_{i=1}^q \left(\mathbb{E}_{\mathbf{f}^*}[p(y_i \leq y_j \forall j \neq i)^2] - \mathbb{E}_{\mathbf{f}^*}[p(y_i \leq y_j \forall j \neq i)]^2 \right), \quad (10)$$

where expectations $\mathbb{E}_{\mathbf{f}^*}[\cdot]$ can be computed by integrating the likelihood of Equation (3) (or its square) over the posterior distribution of the latent values \mathbf{f}^* . Since the equation has no analytic solution, it and its gradients have to be approximated and the minimization faces the same challenges as discussed at the end of the previous section.

3.3 Thompson sampling for batches

A purely exploratory approach does not exploit the information about the known good solutions. EI approaches are known to over-exploit and the proposed approaches are very expensive to compute. Although Thompson sampling is heuristic, it is known to work well in practice and nicely balance between exploration and exploitation [González et al., 2017, Hernández-Lobato et al., 2017]. We use the scalable batch BO approach of Hernández-Lobato et al. [2017] to select the batch locations in our experiments. In practice, we sample q continuous draws from the posterior predictive distribution of the latent variable and select each batch location as a minimum of the corresponding sample. The problem with independent draws is over-exploration of the boundary of the domain [Siivola et al., 2018]. If the uncertainty is large on the boundary or there are boundary minima, many draws from the same batch are more likely to have minimum exactly on the boundary resulting in inefficient use of samples.

3.4 Going beyond the batch winner case

Generalizing the equations beyond the batch winner case only requires updating the parts that contain the likelihood of the batch winner ($p(y_i \leq y_j \forall j \neq i)$) to more general one. For instance in the pure exploration strategy (Section 3.2), we would have to sum the variances of each possible feedback outcome and weight them by their predictive probabilities. This becomes infeasible even for the full ranking feedback with $q!$ options. Thompson sampling for batches requires no change.

Algorithm 1 Pseudo-code of the proposed PBBO method. The inputs are the batch size q , the *stopping criterion*, the *acquisition strategy* and the GP model.

```

1: while stopping criterion is False do
2:   Fit a GP to the available preferential observations
    $\{\mathbf{C}^i\}_{i=1}^N$  at  $\{\mathbf{X}^i\}_{i=1}^N$ .
3:   Find  $q$  locations  $\mathbf{X}^{N+1} = \{\mathbf{x}_i\}_{i=1}^q$  using the acquisition strategy.
4:   Query the preference  $\mathbf{C}^{N+1}$  of  $\mathbf{X}^{N+1}$ .
5:   Augment  $\{\mathbf{X}^i\}_{i=1}^N$  with the preference locations
    $\mathbf{X}^{N+1}$  and  $\{\mathbf{C}^i\}_{i=1}^N$  with the preference outcomes
    $\mathbf{C}^{N+1}$ .
6: end while

```

3.5 Preferential batch Bayesian optimization

The pseudo-code for general acquisition strategy is presented in Algorithm 1. The different parts of the algorithm scales as follows. Assuming N batches of size q , fitting the GP (row 2 in the pseudo code) has the time complexity of $\mathcal{O}((Nq)^3)$. The inference method brings some overhead to this. The computational complexity of optimization of the new batch location has been discussed earlier (see the end of Sections 3.1, 3.2 and 3.3).

4 Experiments

We present three simulated experiments and four real data case studies that extensively show the performance of our model. All results are shown for four different inference methods abbreviated as follows. EP stands for the expectation propagation model presented in the Section 2.4.1. FRVI stands for the full rank variational inference model presented in the Section 2.4.2, Equation (6). MFVI is a mean field version of the previous, Equation (7). Markov chain Monte Carlo (MCMC) is used as a ground truth. As a baseline method, we show results if all acquisitions were selected completely at random, we call this method 'baseline' from here on. The acquisition strategies are abbreviated as follows. q-EI stands for the q-expected improvement, SV stands for the sum of variances and TS stands for Thompson sampling. The methods are implemented on top of the software package GPy [GPy, since 2012] and the MCMC inference is implemented using Stan 2.18.0 [Stan Development Team, 2018]. In all experiments the GP kernel is the squared exponential and the hyper-parameters are fixed to point values by optimizing a regular GP with 2500 noise free observations.

4.1 Effect of the inference method on the acquisition function

The different inference methods approximate the uncertainty differently and this affects how the BO selects the next batch for different acquisition strategies. Figure 1 visualizes the

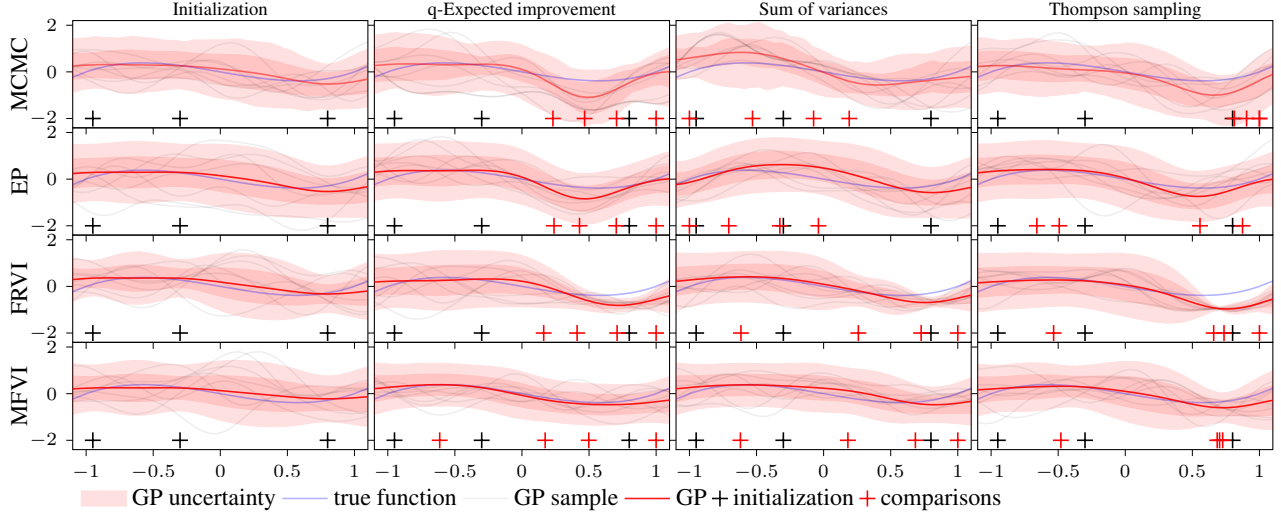


Figure 1: Different rows visualize the true objective and the GP posterior for different inference methods (Markov chain Monte Carlo (MCMC), Expectation propagation (EP), full rank variational inference (FRVI) and mean field variational inference (MFVI)). The first column shows the GP posterior after observing a preferential feedback for a batch of size three (x locations at black '+'-signs). Rest of the columns show the first BO iteration (x locations at red '+'-signs) using different acquisition strategies for a batch size of four. The GP uncertainty is visualized as ± 1 and ± 2 standard deviations. Coinciding comparison locations are visualized with darker '+'-signs.

GP posterior for different inference methods with same training data and then the posterior approximation after the first iteration of BO for all different acquisition strategies. The black box function is

$$f(x) = x^3 - x.$$

The Figure shows that EP and full rank VI result in very similar posteriors as the MCMC ground truth when observing only one batch of preferences that are relatively far away from each other (first column). When observing the second batch through BO (all but first column), EP produces a wider posterior than MCMC, and VI produces a narrower posterior (second and third rows). The Figure also nicely illustrates the differences between the acquisition strategies. q-EI queries at locations with known good values, while SV selects the locations such that the means of the predictive distribution have similar values but the uncertainty of the values is large. Thompson sampling queries at random locations that might have good values resulting in more variation, but the method is likely to sample several locations from the boundary as also mentioned in Section 3.3. More results for different batch sizes and functions can be found in Appendix A4.

4.2 Synthetic functions from the Sigopt function dataset

Sigopt¹ library is a collection of benchmark functions developed to evaluate BO algorithms [Dewancker et al., 2016].

¹Function library available at: <https://github.com/sigopt/evalset>

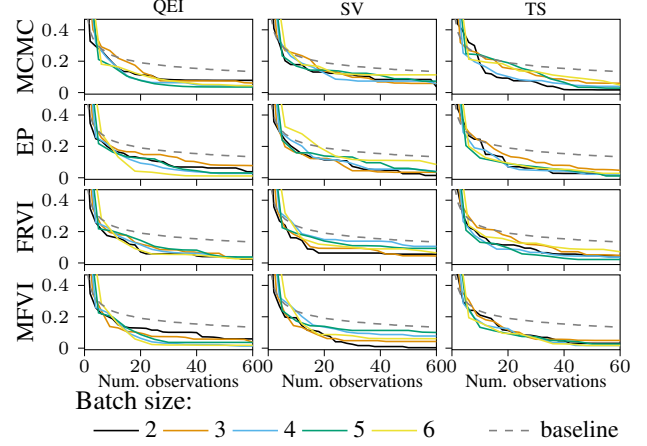


Figure 2: Ursem Waves-function from the Sigopt function library. Each line illustrates the smallest value seen so far as a function of number of observations. The function is scaled between 0 and 1. Different colors in each plot are different batch sizes, rows are different inference methods and columns are different acquisition functions. Each line is a mean of 10 different runs. The dashed black line shows the average performance of the baseline, random search.

Ursem Waves is a function from the library with multiple local minima around the search domain and an absolute minimum on the border. Figure 2 shows the best absolute function value for the locations the function has been evaluated so far as a function of number of function evaluations.

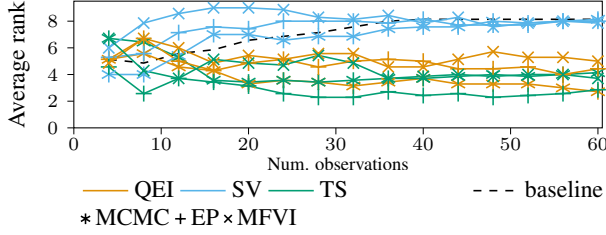


Figure 3: All combinations of the inference methods and acquisition functions are ranked based on their average performance over 10 runs for the batch size of 4 as a function of number of evaluations so far. Each combination is given a rank between 1–10 (lower is better) for each iteration. The figure shows the ranks averaged over 6 functions from the Sigopt library (Ursem Waves, Adjiman, Deceptive, MixtureOfGaussians02 and 3 and 4 dimensional Hartmann-functions). FRVI is not shown due to it performing the worst and to maintain the clarity of the picture. Performance of random search is shown as a baseline.

The results are shown for batch sizes 2–6, three acquisition functions, and 4 inference methods. The shown lines are averaged over 10 random runs. The function evaluations are transformed to batch feedback by evaluating the function for the whole batch at once and returning the minimum as the batch winner. The exact details of how the runs were configured are in Appendix A5.

The results show that all introduced acquisition functions perform better than the baseline, random search. The results show no clear difference between batch sizes for any inference method or acquisition strategy. Similar results as in Figure 2 for five other functions from the Sigopt library can be found from Appendix A5. The biggest difference in these results is that sometimes SV performs worse than the baseline due to it being designed extremely explorative.

Figure 3 shows the average performance of three inference methods (MCMC, EP and MFVI) and all acquisition functions for the batch size of four. The results are averaged over six functions from the Sigopt function library. The results show that TS and q-EI have the best average performance for all inference methods. There are no big differences between the displayed inference methods. FRVI is left out of the picture due to its poor performance caused by it underestimating the uncertainty of the observations. This phenomenon is nicely illustrated on the last row of Figure 1.

4.3 Comparison of batch winner and full ranking

One argument against using the batch winner type feedback in BO is that it is less informative than full ranking. Although it is not always possible to get the full ranking and providing the batch winner is less work for the user, it is interesting to compare how much does less informative feedback affect the

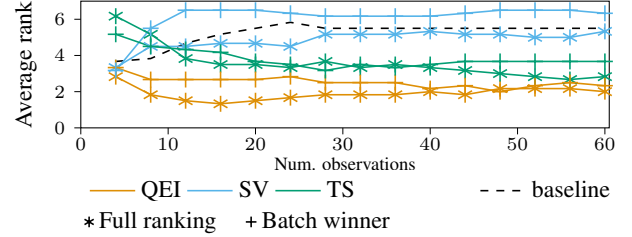


Figure 4: Same as in Figure 3, but for comparing full ranking and batch winner feedbacks.

optimization result. The form of q-EI is identical for batch winner and full ranking. As SV becomes infeasible (sum over $q!$ options), we approximate it with the batch winner form, Equation (10).

Figure 4 shows the average performance of complete ordering and batch winner type feedbacks for all three acquisition functions with batch size four. The results are averaged over six functions from the Sigopt function library. The results show that the full ordering type feedback consistently performs better than the batch winner but the variation in performance is bigger between different acquisition functions than between the two feedback types.

4.4 Real life data case studies

To get insight on how the presented BO approach performs in real life applications, we perform similar experiments with real data as we did in the previous section with the simulated data. As the limitation of the proposed BO approach is the scalability for dimensionality and batch size, we had to stick with low dimensional datasets ($d \leq 4$), where optimization might be a realistic task. No standard datasets for comparing preferential optimization methods yet exists, so we collected 4 different datasets to test the method with. From these datasets, we recovered the full ranking (from best to worst) of the whole dataset (either based on pairwise preferences or direct numerical values) and used that to provide feedback to any batch requested by the tested algorithms. Since real data is discrete, we use linear extrapolation to compute ranking for points that are not in the dataset.

Sushi dataset² has complete ranking of 100 sushi items by humans and 4 continuous features describing each sushi item. In the Candy dataset, an online survey was used to collect 269 000 pairwise preferences to 86 different candies³ with two continuous features, from which it is possible to recover the full ranking of the candies. White wine quality dataset [Cortez et al., 2009] has 4899 white wines with 12

²Sushi dataset available at: <http://www.kamishima.net/sushi/>

³Candy dataset available at: <https://github.com/fivethirtyeight/data/blob/master/candy-power-ranking/candy-data.csv>

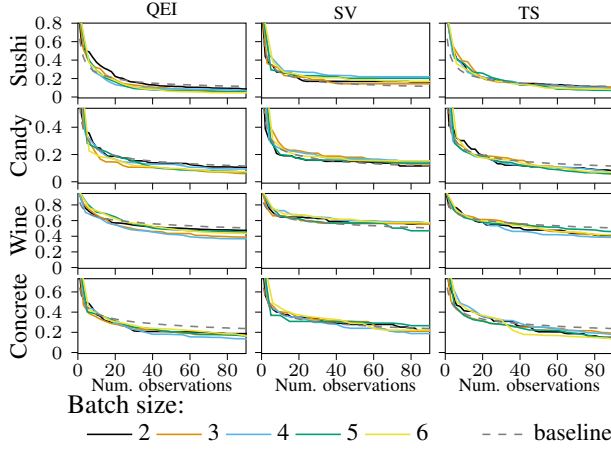


Figure 5: Summary of the performance of the presented method on the real datasets. Each plot illustrates minimum value seen so far as a function of number of function evaluations. All data sets are scaled between 0 and 1. Different colors in plots are different batch sizes, rows are different data sets and columns are different acquisition functions. Each line is a mean of 10 different runs. The dashed black line shows the average performance of the baseline, random search. All lines use EP as an inference method.

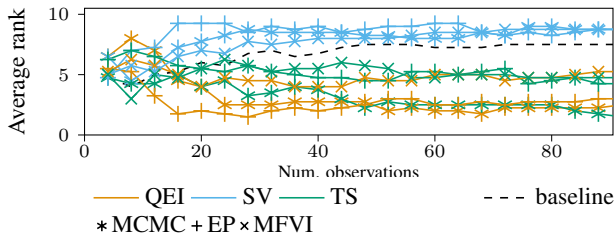


Figure 6: Same as in Figure 3, but for Sushi, Candy, Wine and Concrete datasets.

continuous features and each given a score between 0 and 10. Concrete compressive strength dataset [Yeh, 1998] has 1030 different concrete samples with 8 features and compressive strength is used for ranking. As the White wine quality and Concrete datasets are too high dimensional for our approach to scale, we chose the 4 and 3, respectively, most informative features for the Sushi and Concrete data sets. The features were selected by fitting a GP with squared exponential kernel to the data and by selecting the features with the smallest length scales.

Figure 5 shows the minimum function value seen so far as a function of number of function evaluations. The results show batch sizes 2–6 and three acquisition functions for all 4 datasets when EP is used as an inference function. Each line shows the average over 10 random runs for each setting. Results for rest of the inference methods and the exact details of how the runs were configured are in Appendix A6.

The results are consistent with the results of the synthetic functions from the Sigopt-dataset, with one exception; SV is not able to outperform the baseline for any of the datasets for most batch sizes. Another notable difference compared to the simulated results is that all methods seem to beat the baseline only barely due to the low signal-to-noise ratio in the data. When fitting a GP to the data sets that are scaled between 0–1, the noise standard deviation varies between 0.1–0.2. At maximum 4 dimensions are not enough for modeling the data. The noisiness of the data is more visible for non-expert data sets; Candy and Sushi. Figure 6 shows the average performance of MCMC, EP and MFVI for all three acquisition function over all four real datasets for batch size four. Also here it can be seen that q-EI and TS outperform SV and that EP outperforms MFVI.

5 Conclusion

Our paper extends the existing preferential Bayesian optimization methods to batch setting. This extends the usability of the BO in cases where it is possible to query feedback in the batch setting. These are natural especially in the cases where a human gives feedback to the BO algorithm, such as product design tasks in the food industry. We tested our method with four extensive 1–4 dimensional case studies that illustrate how the batch size, acquisition algorithm and inference method affect to the optimization result.

The results suggest that batch winner feedback is sufficient for optimization tasks as it is easier to collect than full ranking of the batch and it performs almost as well in BO. The results suggest that if the size of the available data is small, the dimensionality is low and the batch size is small, practitioners should use EP inference or MCMC sampling to approximate the posterior distribution. If this is not the case or EP is numerically unstable, the second best option is MFVI due to its robustness and scalability. As acquisition function we recommend Thompson sampling due to its scalability and consistent performance.

We see two potential topics for further research. As the two information theoretically motivated acquisition functions, q-EI and SV, are impractical if either dimensionality or batch size are high, there is room to improve their speed. The second potential topic is to study different forms of batch feedback. We concentrated on the batch winner case, but other forms of feedback might also be interesting for the practitioners, especially as the EP inference and the presented acquisition functions can easily be extended, as discussed in Section 3.4.

References

Eric Brochu. *Interactive Bayesian optimization: learning user preferences for graphics and animation*. PhD thesis, University of British Columbia, 2010.

Peter Brusilovsky, Alfred Kobsa, and Wolfgang Nejdl, editors. *The Adaptive Web: Methods and Strategies of Web Personalization*. Springer Science Business Media, Berlin, Heidelberg, 2007.

Clément Chevalier and David Ginsbourger. Fast computation of the multi-points expected improvement with applications in batch selection. In *Proceedings of the 26th International Conference on Learning and Intelligent Optimization*, pages 59–69, 2013.

Wei Chu and Zoubin Ghahramani. Extensions of Gaussian processes for ranking: semisupervised and active learning. *Proceedings of the Learning to Rank workshop at the 18th Conference on Neural Information Processing Systems*, pages 29–34, 2005a.

Wei Chu and Zoubin Ghahramani. Preference learning with Gaussian processes. In *Proceedings of the 22nd International Conference on Machine Learning*, pages 137–144, 2005b.

Paulo Cortez, António Cerdeira, Fernando Almeida, Telmo Matos, and José Reis. Modeling wine preferences by data mining from physicochemical properties. *Decision Support Systems*, 47(4):547–553, 2009.

Ian Dewancker, Michael McCourt, Scott Clark, Patrick Hayes, Alexandra Johnson, and George Ke. A stratified analysis of Bayesian optimization methods. *arXiv preprint arXiv:1603.09441*, 2016.

Javier González, Zhenwen Dai, Andreas Damianou, and Neil D. Lawrence. Preferential Bayesian optimization. In *Proceedings of the 34th International Conference on Machine Learning*, pages 1282–1291, 2017.

Javier González, Zhenwen Dai, Philipp Hennig, and Neil Lawrence. Batch Bayesian optimization via local penalization. In *Proceedings of the 19th International Conference on Artificial Intelligence and Statistics*, volume 51, pages 648–657, 2016.

GPy. GPy: A Gaussian process framework in python. [http://github.com/SheffieldML/GPy](https://github.com/SheffieldML/GPy), since 2012.

Ralf Herbrich, Tom Minka, and Thore Graepel. Trueskill™: A bayesian skill rating system. In *Proceedings of the 19th Conference on Neural Information Processing Systems*, pages 569–576. 2007.

José Miguel Hernández-Lobato, James Requeima, Edward O Pyzer-Knapp, and Alán Aspuru-Guzik. Parallel and distributed thompson sampling for large-scale accelerated exploration of chemical space. *arXiv preprint arXiv:1706.01825*, 2017.

Jonathan Ho and Stefano Ermon. Generative adversarial imitation learning. In *Proceedings of the 29th Conference on Neural Information Processing Systems*, pages 4565–4573. 2016.

Donald R. Jones. A taxonomy of global optimization methods based on response surfaces. *Journal of global optimization*, 21(4):345–383, 2001.

Daniel Kahneman and Amos Tversky. Prospect theory: An analysis of decision under risk. *Econometrica*, 47(2):263–91, 1979.

Diederik P Kingma and Max Welling. Auto-encoding variational Bayes. *arXiv preprint arXiv:1312.6114*, 2013.

Thomas P Minka. Expectation propagation for approximate Bayesian inference. In *Proceedings of the 17th conference on Uncertainty in Artificial Intelligence*, pages 362–369. Morgan Kaufmann Publishers Inc., 2001.

Jonas Močkus. On Bayesian methods for seeking the extremum. In *Proceedings of the 28th Optimization Techniques IFIP Technical Conference*, pages 400–404, 1975.

Manfred Opper and Cédric Archambeau. The variational Gaussian approximation revisited. *Neural computation*, 21(3):786–792, 2009.

Manfred Opper and Ole Winther. Gaussian processes for classification: Mean-field algorithms. *Neural Computation*, 12(11):2655–2684, 2000.

Carl Edward Rasmussen and Christopher KI Williams. *Gaussian processes for machine learning*. The MIT Press, 2nd edition, 2006.

Eero Siivola, Aki Vehtari, Jarno Vanhatalo, Javier González, and Michael Riis Andersen. Correcting boundary over-exploration deficiencies in Bayesian optimization with virtual derivative sign observations. In *Proceedings of the 28th International Workshop on Machine Learning for Signal Processing*, pages 1–6, 2018.

Jasper Snoek, Hugo Larochelle, and Ryan P. Adams. Practical Bayesian optimization of machine learning algorithms. In *Proceedings of the 25th Conference on Neural Information Processing Systems*, pages 2951–2959, 2012.

Stan Development Team. The Stan Core Library, 2018. URL <http://mc-stan.org/>. Version 2.18.0.

Yanan Sui, Vincent Zhuang, Joel W Burdick, and Yisong Yue. Multi-dueling bandits with dependent arms. *arXiv preprint arXiv:1705.00253*, 2017.

Richard S. Sutton and Andrew G. Barto. *Introduction to Reinforcement Learning*. The MIT Press, 1st edition, 1998.

Michalis K. Titsias. One-vs-each approximation to softmax for scalable estimation of probabilities. In *Proceedings of the 29th Conference on Neural Information Processing Systems*, pages 4161–4169, 2016.

Carlos Villacampa-Calvo and Daniel Hernández-Lobato. Scalable multi-class Gaussian process classification using expectation propagation. In *Proceedings of the 34th International Conference on Machine Learning*, pages 3550–3559, 2017.

I-Cheng Yeh. Modeling of strength of high-performance concrete using artificial neural networks. *Cement and Concrete research*, 28(12):1797–1808, 1998.

Yisong Yue and Thorsten Joachims. Interactively optimizing information retrieval systems as a dueling bandits problem. In *Proceedings of the 26th Annual International Conference on Machine Learning*, pages 1201–1208, 2009.

Yisong Yue, Josef Broderb, Robert Kleinbergc, and Thorsten Joachims. The k -armed dueling bandits problem. *Journal of Computer and System Sciences*, 78(5):1538 – 1556, 2012.

Preferential Batch Bayesian Optimization: Supplementary Material

E1 Explaining the high computational cost of pq-EI

As we further open Equation (8), it becomes:

$$\begin{aligned} \text{pq-EI} &= \mathbb{E}_{\mathbf{y}, \mathbf{y}_{min}} \left[\left(\max_{i \in [1, \dots, q]} (y_{min} - y_i) \right)_+ \right] \\ &= \int_{-\infty}^{\infty} p(y_{min}) \sum_{i=1}^q \mathbb{E}_{\mathbf{y}} (y_{min} - y_i | y_i \leq y_{min}, y_i \leq y_j \forall j \neq i, y_{min}) \times p(y_i \leq y_{min}, y_i \leq y_j \forall j \neq i | y_{min}) dy_{min}, \end{aligned}$$

where $p(y_{min})$ is the distribution of minimum of $p \times q$ dimensional Normal distribution⁴ (p is number of iterations before this and q is the batch size). More explicitly

$$p(y_{min}) = \sum_{i=1}^p \sum_{j=1}^q N(-y_{min} | -\mu_{ij}, \Sigma_{ij}^{-1}) \Phi_{pq-1}(-y_{min} \mathbf{1} | -\boldsymbol{\mu}_{-ij}(y_{min}), \Sigma_{-ij}^{-1}) ,$$

where μ_{ij} is the posterior mean of the latent function at i :th batch and j :th batch location, Σ_{ij}^{-1} is the posterior covariance of predictive output at the same location and

$$\boldsymbol{\mu}_{-ij}(y_{min}) = \boldsymbol{\mu}_{-ij} - (y_{min} - \mu_{ij}) \Sigma_{-ij}^{-1} / \Sigma_{ij}^{-1}, \text{ and } \Sigma_{-ij}^{-1} = \Sigma_{-ij}^{-1} - \Sigma_{-ij}^{-1} \Sigma_{ij}^{-1} \Sigma_{-ij}^{-1} / \Sigma_{ij}^{-1}.$$

Furthermore $\mathbb{E}_{\mathbf{y}} (y_{min} - y_i | y_i \leq y_{min}, y_i \leq y_j \forall j \neq i, y_{min})$ can be computed efficiently with Tallis formula for small batch sizes. However, even though we need to only perform numerical integration over one dimension (as multidimensional cumulative normal distributions can efficiently be approximated), the computation of $p(y_{min})$ becomes computationally very demanding because of the need for computation of very high dimensional cumulative normal distribution functions ($pq - 1$ becomes very large after few iterations).

E2 Copeland Expected Improvement for batches

Soft Copeland score of an outcome can be computed as

$$S(\mathbf{x}) = \frac{1}{\text{Vol}(\mathcal{X})} \int_{\mathbf{x}' \in \mathcal{X}} p(y(\mathbf{x}) \leq y(\mathbf{x}')) d\mathbf{x}' = \frac{1}{\text{Vol}(\mathcal{X})} \int_{\mathbf{x}' \in \mathcal{X}} \phi \left(\frac{\mu(\mathbf{x}') - \mu(\mathbf{x})}{2\sigma^2 + \sigma^2(\mathbf{x}) + \sigma^2(\mathbf{x}')} \right) d\mathbf{x}'.$$

Since the joined distribution of soft Copeland scores doesn't follow multivariate normal, the expected improvement needs to be computed by recomputing the model posterior for all possible feedback outcomes of the batch,

$$\text{cq-EI} = \sum_{i=1}^q p(y_i \leq y_j \forall j \neq i) (S(\mathbf{x}_i | y_i \leq y_j \forall j \neq i) - S_{min}).$$

Computing cq-EI is computationally heavy, since it requires performing q times one model update and one d -dimensional numerical integral. However, this cost stays constant for all iterations and might thus make it practical for some problems.

⁴Arellano-Valle, R. B., and Genton, M. G. (2008). On the exact distribution of the maximum of absolutely continuous dependent random variables. *Statistics & Probability Letters*, 78(1), 27-35.

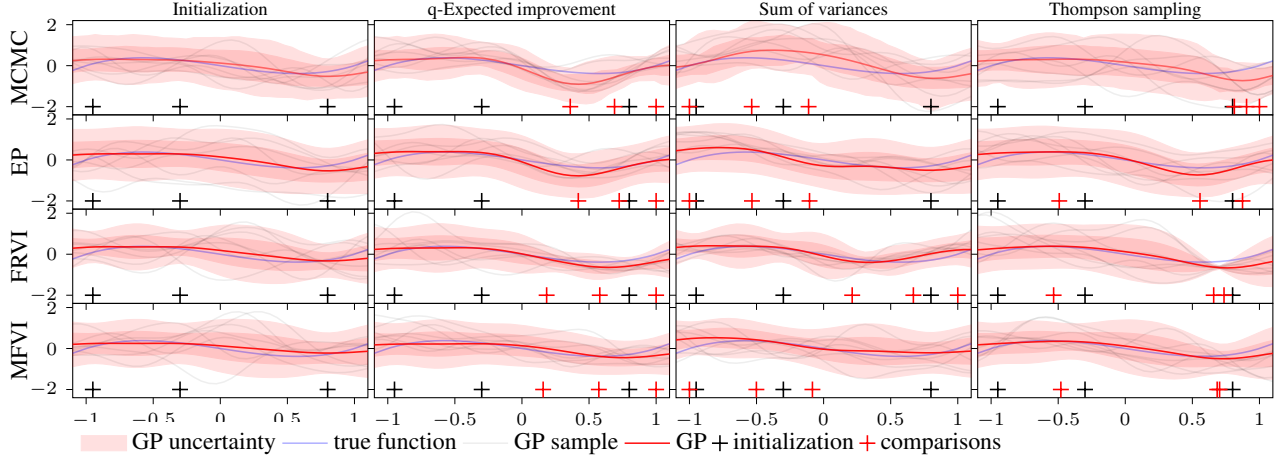


Figure 7: Same as in Figure 1, but for batch size 3.

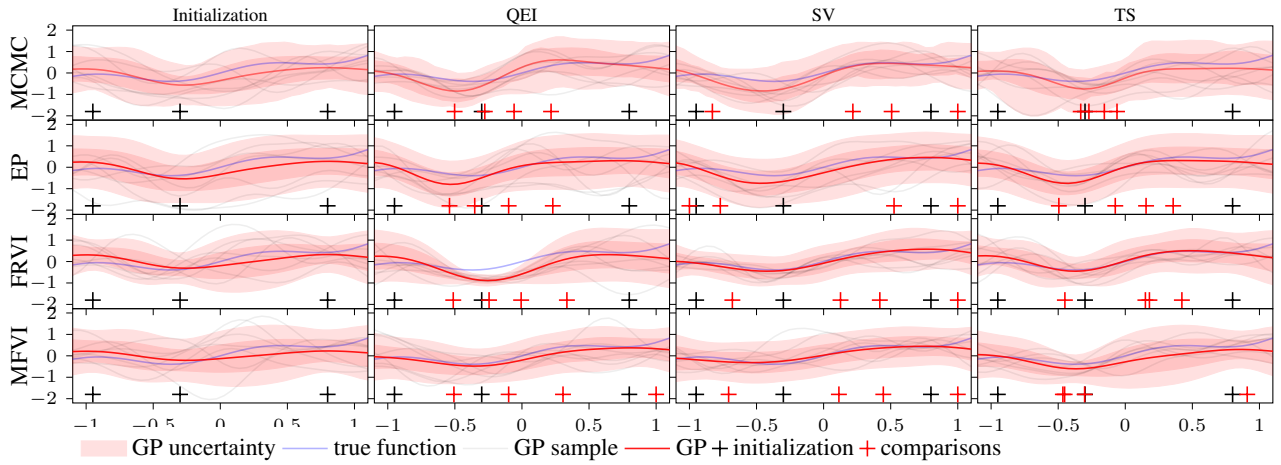


Figure 8: Same as in Figure 1, but for different function.

E3 Sampling from where the output is uncertain does not lead to exploration

When the feedback is given as preferences, exploration can be thought in many ways. As discussed by González *et al.* (2016), if the uncertainty is thought as the uncertainty of the outcome of the comparison, the probability of the outcome of comparisons can be modeled as a categorical distribution. If uncertainty is modeled with Shannon entropy,

$$\sum_i p(y_i \leq y_j \forall j \neq i) \log(p(y_i \leq y_j \forall j \neq i)),$$

the maximum Entropy is gained when the probabilities $p(y_i \leq y_j \forall j \neq i)$ are equal, which is true when $y_i \approx y_j \forall i, j$. This allows sampling also from areas already in the dataset, assuming that the values are close to each other.

E4 Details and additional results for Section 4.1

Figure 7, presents same experiment as in Section 4.1, but for batch size of 6. Figures 8 and 9 have results for function $\frac{1}{4} \sin(5x) + \frac{1}{2}e^x - \frac{1}{2}$.

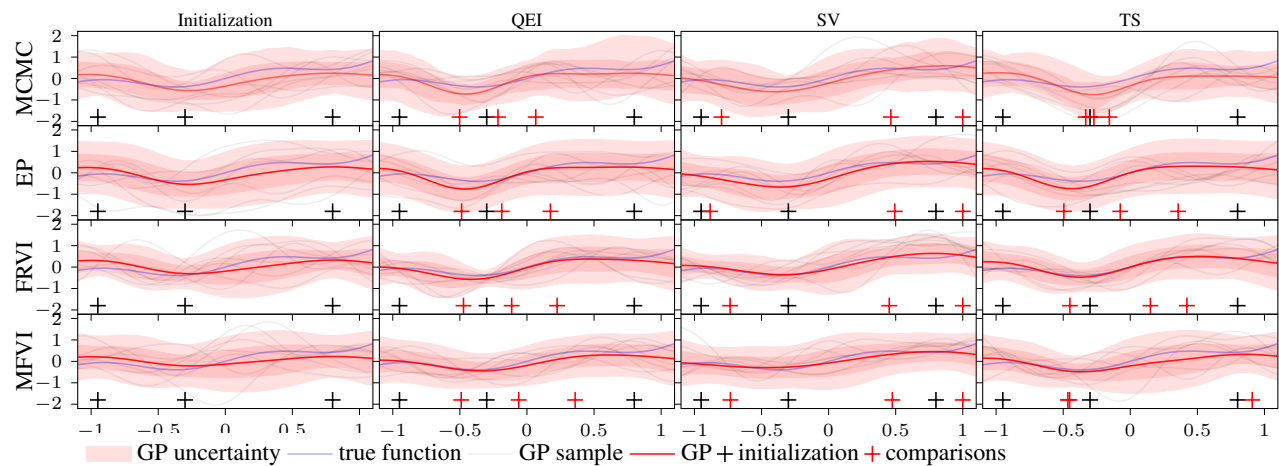


Figure 9: Same as in Figure 1, but for batch size 3 and for different function.

E5 Details and additional results for Section 4.2

For all simulation runs, the function bounds and output was scaled between 0 and 1, for all dimensions. The batch feedbacks were computed from outputs which were corrupted with noise that has standard deviation of 0.05. q-EI and SV were computed with 5000 posterior samples. All acquisition functions were optimized using limited memory Broyden–Fletcher–Goldfarb–Shanno (BFGS) algorithm with box constraints. The optimization was restarted 30 times for q-EI and SV. To increase the robustness of the EP, we do not allow distances between points to be less than 0.05 within a single batch. The numerical gradients of TS were computed with $\delta = 10^{-5}$ and only 100 closest samples were taken into account when conditioning on the evaluated samples. Optimization of EP was limited to at maximum 100 iterations. Optimization of MFVI and FRVI was limited to 50 iterations and Adam was used for optimization.

Figure 10 presents similar results as in Section 4.2 for the 5 other functions from the Sigopt function library. All these functions are well known global optimization bench mark functions.

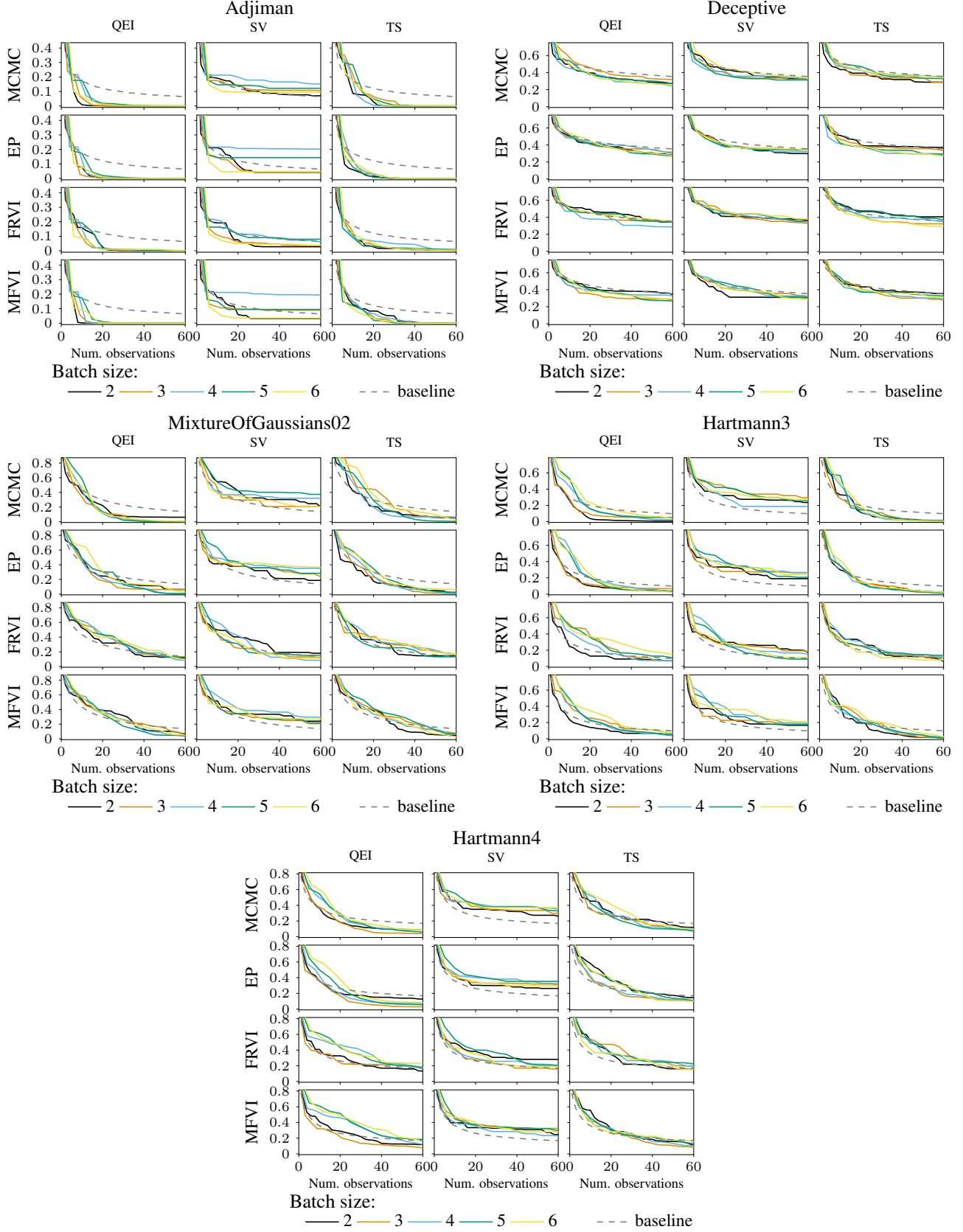


Figure 10: Same as in Figure 2, but for Adjiman, Deceptive, MixtureOfGaussians02 and 3 and 4 dimensional Hartmann functions from the Sigopt function library.

E6 Additional results for Section 4.3

Additional results for the experiments in Section 4.3. Figure 11 compares full ranking and batch winner feedbacks for six functions from the Sigopt library for q-EI, TS and SV for batch sizes 3–6.

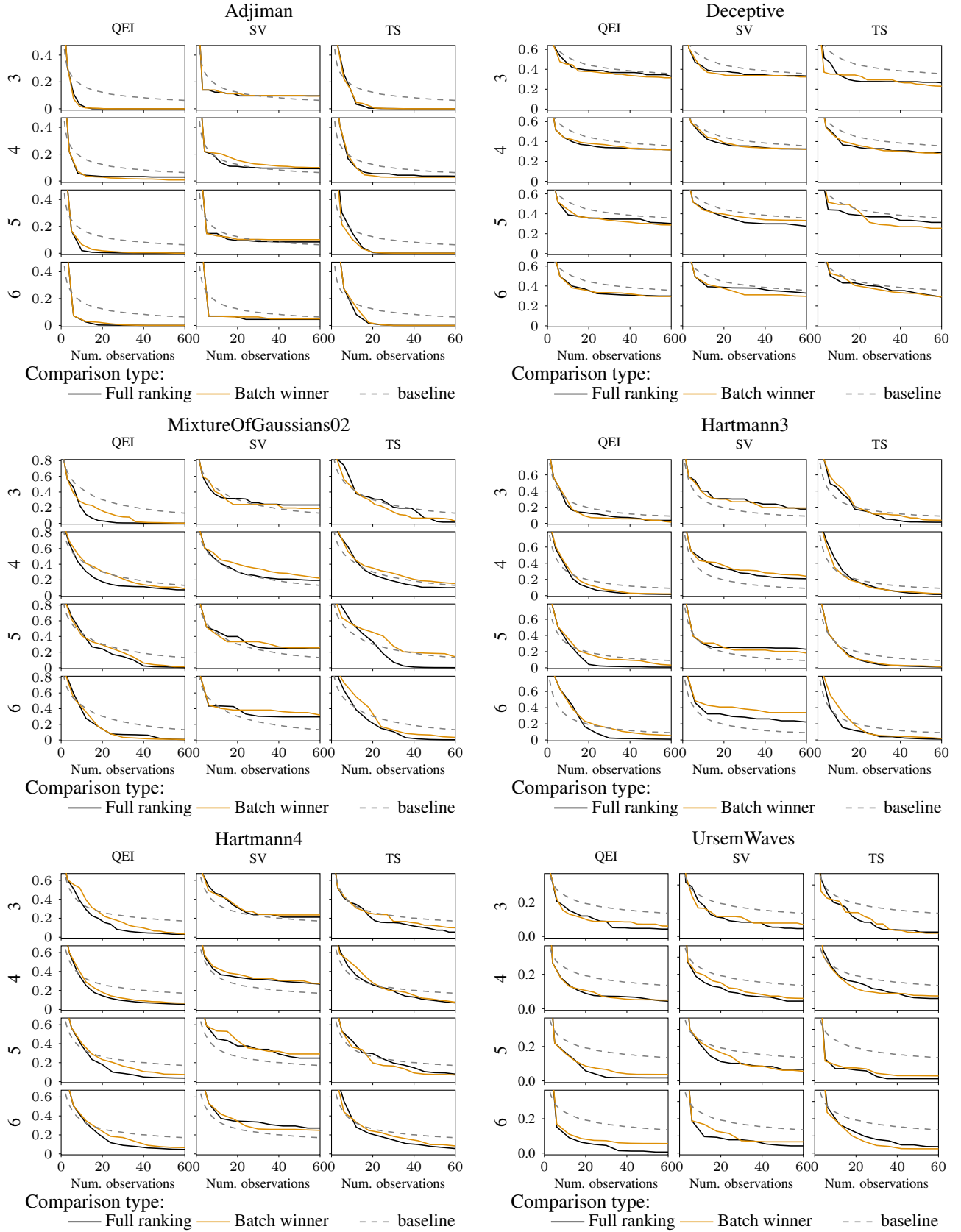


Figure 11: Comparison of full ranking and batch winner feedbacks for six functions from the Sigopt function for the tree acquisition functions and batch sizes 3–6.

E7 Additional results for Section 4.4

The details of the experiments are the same as for the experiments in Section 4.4 with few exceptions. Since the functions are higher dimensional, acquisition optimization for q-EI and SV was restarted 60 times. Also, no noise was added to real data.

Figure 12 presents similar results as in Section 4.4 for the 3 other inference methods.

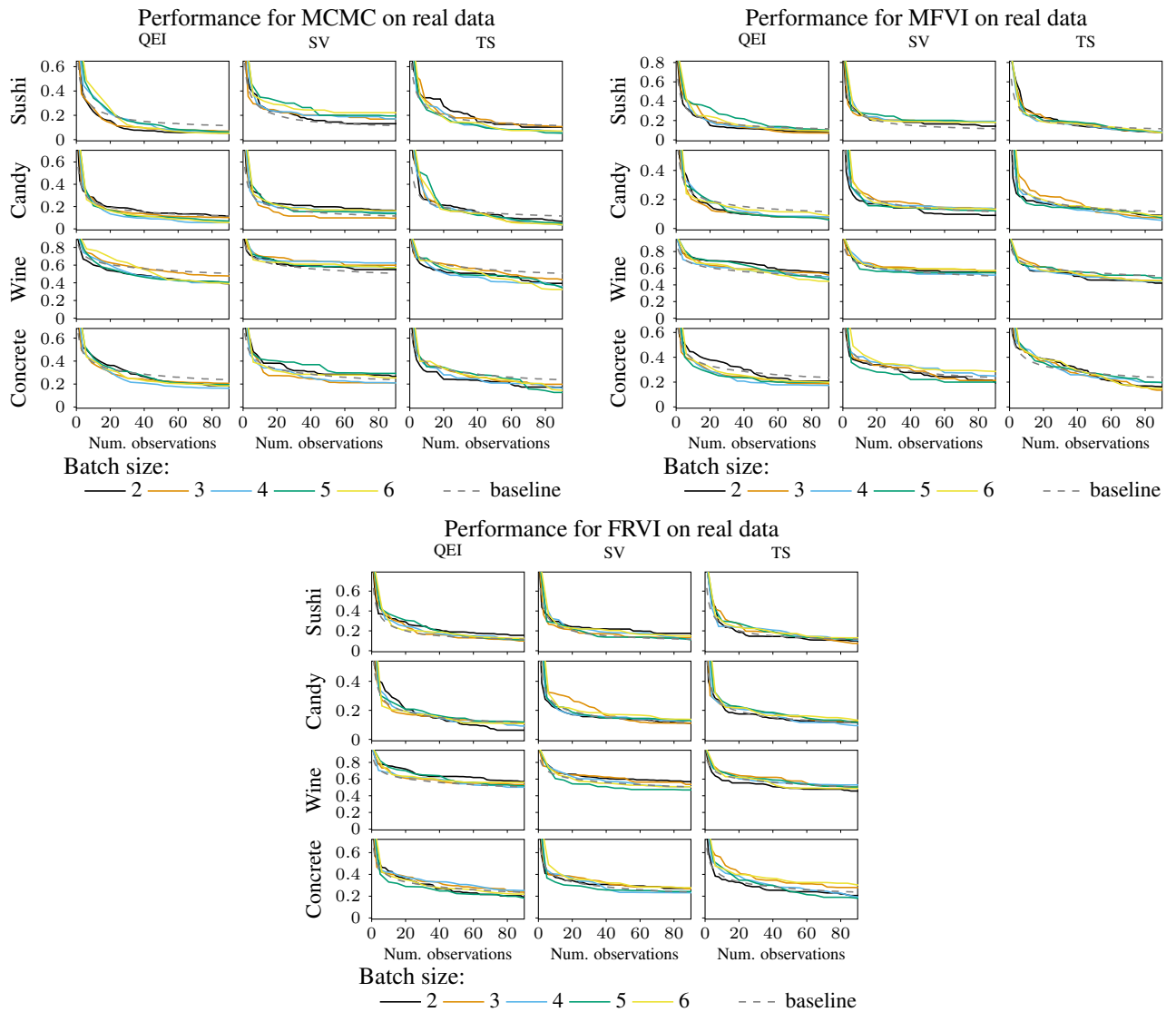


Figure 12: Performances of MCMC, MFVI and FRVI inferences on the real data.